Article

Neuron

Locomotion, Theta Oscillations, and the Speed-Correlated Firing of Hippocampal Neurons Are Controlled by a Medial Septal Glutamatergic Circuit

Highlights

- Locomotion is initiated and controlled by the firing of medial septal VGluT2$^+$ neurons
- These neurons couple theta oscillations and CA1 activity to locomotion speed
- CA1 activity increase is achieved by speed-dependent disinhibition of CA3 and EC input
- MSDB VGluT2$^+$ neurons mediate the brain state transition associated with locomotion

Authors

Falko Fuhrmann, Daniel Justus, ..., Martin Fuhrmann, Stefan Remy

Correspondence

stefan.remy@dzne.de

In Brief

Fuhrmann et al. identify a glutamatergic medial septal circuit that controls the initiation and velocity of locomotion. This circuit mediates the pre-motor initiation of theta oscillations and, via hippocampal disinhibition, underlies the locomotion speed dependence of hippocampal neuronal firing rates.

Fuhrmann et al., 2015, Neuron *86*, 1253–1264
June 3, 2015
http://dx.doi.org/10.1016/j.neuron.2015.05.001

CellPress

Neuron
Article

Locomotion, Theta Oscillations, and the Speed-Correlated Firing of Hippocampal Neurons Are Controlled by a Medial Septal Glutamatergic Circuit

Falko Fuhrmann,[1,6] Daniel Justus,[1,6] Liudmila Sosulina,[1] Hiroshi Kaneko,[1] Tatjana Beutel,[1] Detlef Friedrichs,[1] Susanne Schoch,[2,3] Martin Karl Schwarz,[4] Martin Fuhrmann,[5] and Stefan Remy[1,2,*]
[1]Neuronal Networks Group, German Center for Neurodegenerative Diseases, Ludwig-Erhard-Allee 2, 53175 Bonn, Germany
[2]Department of Epileptology
[3]Section of Translational Epilepsy Research, Department of Neuropathology
University of Bonn Medical Center, Sigmund-Freud Strasse 25, 53127 Bonn, Germany
[4]Functional Neuroconnectomics Group, Department of Epileptology, Life & Brain Center, University of Bonn, Medical School, Sigmund-Freud Strasse 25, D-53105 Bonn, Germany
[5]Neuroimmunology and Imaging Group, German Center for Neurodegenerative Diseases, Ludwig-Erhard-Allee 2, 53175 Bonn, Germany
[6]Co-first author
*Correspondence: stefan.remy@dzne.de
http://dx.doi.org/10.1016/j.neuron.2015.05.001

SUMMARY

Before the onset of locomotion, the hippocampus undergoes a transition into an activity-state specialized for the processing of spatially related input. This brain-state transition is associated with increased firing rates of CA1 pyramidal neurons and the occurrence of theta oscillations, which both correlate with locomotion velocity. However, the neural circuit by which locomotor activity is linked to hippocampal oscillations and neuronal firing rates is unresolved. Here we reveal a septo-hippocampal circuit mediated by glutamatergic (VGluT2$^+$) neurons that is activated before locomotion onset and that controls the initiation and velocity of locomotion as well as the entrainment of theta oscillations. Moreover, via septo-hippocampal projections onto alveus/oriens interneurons, this circuit regulates feedforward inhibition of Schaffer collateral and perforant path input to CA1 pyramidal neurons in a locomotion-dependent manner. With higher locomotion speed, the increased activity of medial septal VGluT2 neurons is translated into increased axo-somatic depolarization and higher firing rates of CA1 pyramidal neurons.

INTRODUCTION

During locomotion, CA1 pyramidal neurons integrate multimodal sensory information about environmental stimuli (Andersen, 2007). At higher speed of locomotion, the integration time window in which sensory cue-related information can be associated to a spatial position is substantially narrower than at slower speed. However, even at high velocities, correct associations must be made and rapid navigation has to be based on the correct retrieval of spatial associations from memory. A strategy to compensate for such a "cue-sampling problem" is increasing the neuronal sensitivity to input during locomotion, which would result in increased firing rates and a higher probability of coincident pre- and postsynaptic firing. Indeed, it has been shown that CA1 pyramidal neurons almost linearly increase their firing rates with the velocity of locomotion (Czurkó et al., 1999; Ekstrom et al., 2001; McNaughton et al., 1983). However, the mechanisms underlying the increase of pyramidal neuron firing rates that occurs with the change of the brain-state from resting to locomotor activity are still obscure.

Already several hundred milliseconds before rodents engage in locomotion, a predominant oscillation in the theta frequency band emerges in the hippocampal field potential that can predict the upcoming onset of locomotion (Green and Arduini, 1954; Vanderwolf, 1969; Whishaw and Vanderwolf, 1973). Hippocampal theta oscillations are continuously present during ongoing locomotion and represent a brain-state specialized for processing of spatially related input (Buzsáki, 2002; Buzsáki et al., 1983; Vanderwolf, 1969). In addition, a correlation of theta frequency/power with locomotion velocity has been found (McFarland et al., 1975).

Key regulators of locomotion-related theta oscillations are the medial septal nucleus and the diagonal band of Broca (MSDB) (Buzsáki, 2002; Stumpf et al., 1962). Therefore, we hypothesized that septo-hippocampal projections might be crucially involved in the mechanisms by which CA1 pyramidal neurons increase their firing rates during locomotion.

The three main septo-hippocampal projections are GABAergic (Freund and Antal, 1988), cholinergic (Frotscher and Léránth, 1985), and glutamatergic (Colom et al., 2005; Köhler et al., 1984) and almost exclusively target interneurons of the hippocampal formation (Léránth and Frotscher, 1987; Tóth et al., 1997). Although vesicular glutamate transporter 2-positive glutamatergic neurons (VGluT2 neurons) are an important source of synaptic excitation within the MSDB (Huh et al., 2010; Leão et al., 2015; Manseau et al., 2005), almost nothing is known about their function during behavior. If these glutamatergic neurons were integrated into locomotor circuitry, their proposed excitatory synaptic

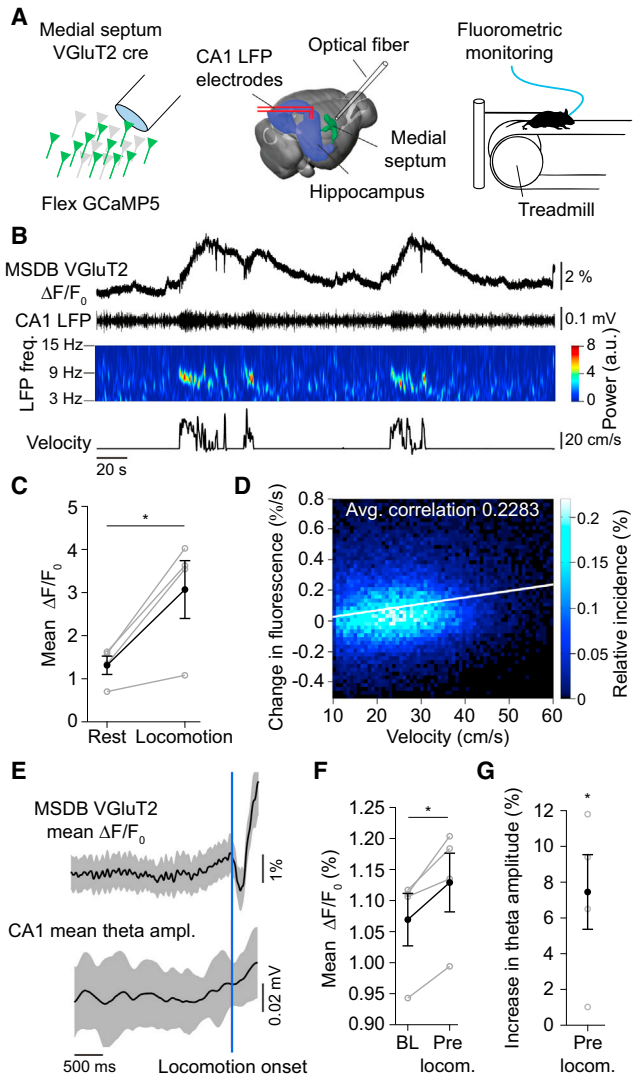

Figure 1. MSDB VGluT2 Neuronal Activity Increases before the Onset of Voluntary Locomotion along with Hippocampal Theta Amplitude and It Correlates with the Locomotion Velocity

(A) Recording configuration.

(B) Representative recording of MSDB VGluT2 population GCaMP5 fluorescence, hippocampal LFP, and velocity.

(C) Increased mean VGluT2 fluorescence during locomotion (individual mouse data are presented in gray, n = 4 mice, mean values ± SEM).

(D) Positive correlation of GCaMP5 fluorescence slope and velocity.

(E) Mean GCaMP5 fluorescence and hippocampal theta amplitude before locomotion onset (gray areas denote SD, n = 4 mice). A small motion artifact (dip in fluorescence) followed the initiation of locomotion.

(F) Mean fluorescence increases in the 100 ms pre-locomotion interval compared to baseline (n = 4 mice, mean values ± SEM).

(G) Increased hippocampal theta amplitude before locomotion onset (n = 4 mice, mean values ± SEM).

Also see Figure S1.

transmission onto other medial septal cell types could contribute to the initiation of theta oscillations, while their septo-hippocampal projections onto CA1 interneurons could allow for modulation of hippocampal microcircuits in a locomotion-dependent manner. Thus, MSDB VGluT2 neurons may represent a missing mechanistic link coupling neuronal firing rates and theta oscillations to movement velocity.

Here, we cell-type specifically monitored the Ca^{2+} activity of MSDB VGluT2 neurons during locomotion and optogenetically stimulated these neurons during single-cell whole-cell patch-clamp and population two-photon imaging of CA1 pyramidal neurons in awake head-fixed mice. We found locomotion-correlated activity of both MSDB VGluT2 neurons and CA1 pyramidal neurons. Combining mono-transsynaptic retrograde tracing and brain slice electrophysiology, our findings reveal a disinhibitory mechanism that facilitates the synaptic integration of Schaffer collateral and perforant path input by CA1 pyramidal neurons during the brain-state transition from resting to locomotion.

Locomotion-related firing of VGluT2 septo-hippocampal projections resulted in alveus/oriens (A/O) interneuron-mediated suppression of Schaffer collateral and perforant path feedforward inhibition already before locomotion onset. Through this mechanism, the velocity-dependent activity of MSDB VGluT2 neurons is translated into increased axo-somatic depolarization and higher firing rates of hippocampal CA1 pyramidal neurons during locomotion.

Moreover, we provide in vivo evidence for a key role of MSDB VGluT2 neurons in the pre-motor control of locomotion. Firing of MSDB VGluT2 not only resulted in reliable initiation of locomotion, but the firing rate and number of activated VGluT2 neurons directly controlled the speed and the duration of locomotion. The pre-motor activity of MSDB VGluT2 neurons predicted the speed and delay to onset of the upcoming movement. In parallel, the pre-motor activation of MSDB VGluT2 neurons led to reliable entrainment of hippocampal theta oscillations before locomotion onset. Thus, the firing of MSDB VGLuT2 neurons actively initiated the brain-state transition from resting to locomotion. It mechanistically linked locomotion with theta oscillations and the speed-related regulation of hippocampal CA1 pyramidal neuron firing rates.

RESULTS

MSDB VGluT2 Neurons Are Active before and during Locomotion

We performed fluorometric monitoring of the population activity of MSDB VGluT2 neurons in head-fixed mice on a linear treadmill using cre-recombinase-dependent cell-type-specific expression of the genetically encoded Ca^{2+} indicator GCaMP5 (Figure 1A; Experimental Procedures). We simultaneously recorded the locomotion velocity, the local CA1 hippocampal field potentials, and MSDB-VGluT2-GCaMP5 fluorescence (Figure 1B). Locomotion-related theta oscillations with an average frequency of 7.04 Hz could be reliably observed in area CA1 (Figure 1B and Figures S1C–S1E). We found that the mean $\Delta F/F_0$ recorded in MSDB VGluT2 neurons was significantly higher during locomotion than during resting phases, indicating a locomotion-dependent regulation of the VGluT2 neuronal activity (Figure 1C). Furthermore, the slope of the rising phase of the GCaMP5 fluorescence positively correlated with the velocity of locomotion, indicating higher MSDB VGluT2 activity at higher velocities (Figure 1D). The increase of fluorescence preceded the onset of

locomotion by several hundred milliseconds, suggesting that VGluT2 neurons were recruited during the movement initiation process (Figures 1E and 1F). Likewise, the onset of locomotion-related theta oscillations occurred prior to movement onset (Figures 1E and 1G).

Firing of MSDB VGluT2 Neurons Actively Controls the Speed and Onset of Locomotion and Entrains Hippocampal Theta Oscillations

The majority of medial septal neurons displays theta-burst firing patterns during locomotion (King et al., 1998). To understand the role of MSDB-VGluT2 neurons during the initiation of locomotion and theta oscillations, we performed cell-type-specific stimulation of MSDB-VGluT2 ChR2-expressing neurons via the implanted light fiber at frequencies covering the theta range (from 3 Hz to 12 Hz; Figure S2; Experimental Procedures). The stimulation of MSDB VGluT2 neurons resulted in the initiation of stimulus-locked theta field potential oscillations in CA1 (Figure 2A). These induced hippocampal oscillations almost exactly mirrored the stimulation frequency of MSDB-VGluT2 ChR2-expressing neurons (Figure 2B). In addition, all mice initiated and maintained locomotion during VGluT2-ChR2 theta stimulation (Figure 2C). No changes in either LFP or locomotion properties were observed with 561 nm stimulation (Figure S2J). The characteristics of induced locomotion depended on the frequency of VGluT2-ChR2 neuron firing. The maximal running velocity increased with higher firing frequencies, while the time to locomotion onset showed a negative dependence on the frequency of firing (Figures 2D and 2E; Movie S1). Furthermore, we found that increasing the number of action potentials per burst and the total number of recruited VGluT2 neurons both augmented the reliability of locomotion initiation and the maximal velocity, while the delay to locomotion initiation decreased (Figures S2E and S2F). Reducing the stimulation frequency during ongoing 9 Hz-stimulated locomotion (to 6 Hz) resulted in a respective reduction of locomotion velocity, which returned to initial values when the frequency was returned to 9 Hz (Figure 2F).

It has been suggested that changes of theta frequency and power can predict subsequent behavioral changes (Vanderwolf, 1969; Wyble et al., 2004). We found that even brief sub-second episodes of MSDB-VGluT2/ChR2-firing were sufficient to initiate locomotion (Figure S2G). These brief stimulations led to entrainment of locomotion-related theta oscillations, which persisted even in the absence of stimulation and were continuously present during the time lag between the end of stimulation and the successful movement initiation (Figures 2G–2I). When we locally applied NBQX/D-AP5 within the MSDB to block glutamatergic transmission (Experimental Procedures; Figure S2H), we observed a pronounced reduction of the theta amplitude (by 30%–57%, see Figure 2J and Figure S2I). Thus, VGluT2-mediated excitation of other (synaptically connected) medial septal cell populations contributed predominantly to CA1 theta field oscillations. This finding was not unexpected, since a role of MSDB GABAergic neurons in the pacing of theta oscillations has been found (Freund and Antal, 1988; Hangya et al., 2009). However, in the presence of NBQX/D-AP5 not only the correlation between theta frequency and locomotion velocity that we had observed in the unstimulated intervals was lost (Figures 2K and 2L), but also the effects of VGluT2 neurons on locomotion and theta oscillations were effectively decoupled, because during the blockade of theta oscillations by NBQX/D-AP5, we still observed reliable initiation of locomotion. (Figure S2I). Thus, we concluded that MSDB VGluT2 neurons were indeed the main effector cells of locomotion and played a key role in the initiation of hippocampal theta oscillations, which were transmitted to the hippocampus by the concerted action of $VGluT2^+$ and other MSDB cell types.

Integration of MSDB VGluT2 Neurons into Locomotor Circuitry

Stimulation-induced initiation of locomotion, theta oscillations, or both has been described for several diencephalic (posterior hypothalamus, supramammillary nucleus) and mesencephalic (pontine) locomotor regions (Bland and Oddie, 2001). To probe whether some of these regions selectively project onto MSDB VGluT2 neurons, we performed modified rabies virus-dependent retrograde mono-transsynaptic tracing. Our data are consistent with monosynaptic input neurons in several hypothalamic subregions and the median raphe nuclei (Table 1; Figures S6A–S6H). Immunohistochemical detection of eYFP-containing MSDB VGluT2 efferent projections was consistent with a high density of axons in the ventral tegmental area (VTA), median raphe nuclei, and several hypothalamic nuclei (Figures S6I–S6K), confirming an afferent and efferent integration of MSDB VGluT2 neurons into a more extended theta synchronizing and locomotion promoting circuitry (Bland and Oddie, 2001).

MSDB VGluT2 Activity Translates into Axo-Somatic Depolarization and Increased Firing Rates of CA1 Pyramidal Neurons

A prominent bundle of efferent glutamatergic axons has been shown to project to the hippocampal formation via the fornix. Since the in vivo function of these projections is unknown, we next studied the function of MSDB VGluT2 septo-hippocampal projections on hippocampal processing during locomotion. We investigated synaptic integration of hippocampal CA1 principal cells with subthreshold resolution using combined CA1 LFP and whole-cell recordings during locomotion to understand the mechanisms by which a speed-dependent regulation of CA1 pyramidal neuron firing (Ekstrom et al., 2001; McNaughton et al., 1983) is achieved. At resting potential, VGluT2-ChR2 stimulation in the medial septum consistently evoked a repetitive, summating subthreshold depolarization of the membrane potential consistent with an increased integration of excitatory synaptic input (Figures 3A–3C). In response to this depolarizing input, CA1 pyramidal neurons showed an increased firing of stimulus-locked action potentials/bursts (Figures 3D and 3E). We then altered the stimulation frequencies and observed a frequency-dependent increase of both the peak and mean depolarization (Figures 3F–3H), further supporting that the regulation of CA1 pyramidal neuron firing rates may occur on the level of synaptic integration.

We next tested whether the locomotion speed-dependent activity increase could be detected on the population activity level of CA1 hippocampal neurons. Therefore, we monitored the activity of more than 1,000 neurons using two-photon Ca^{2+} imaging through a chronic hippocampal window (Figure 4B). We found a positive dependence of the number of detected Ca^{2+} transients

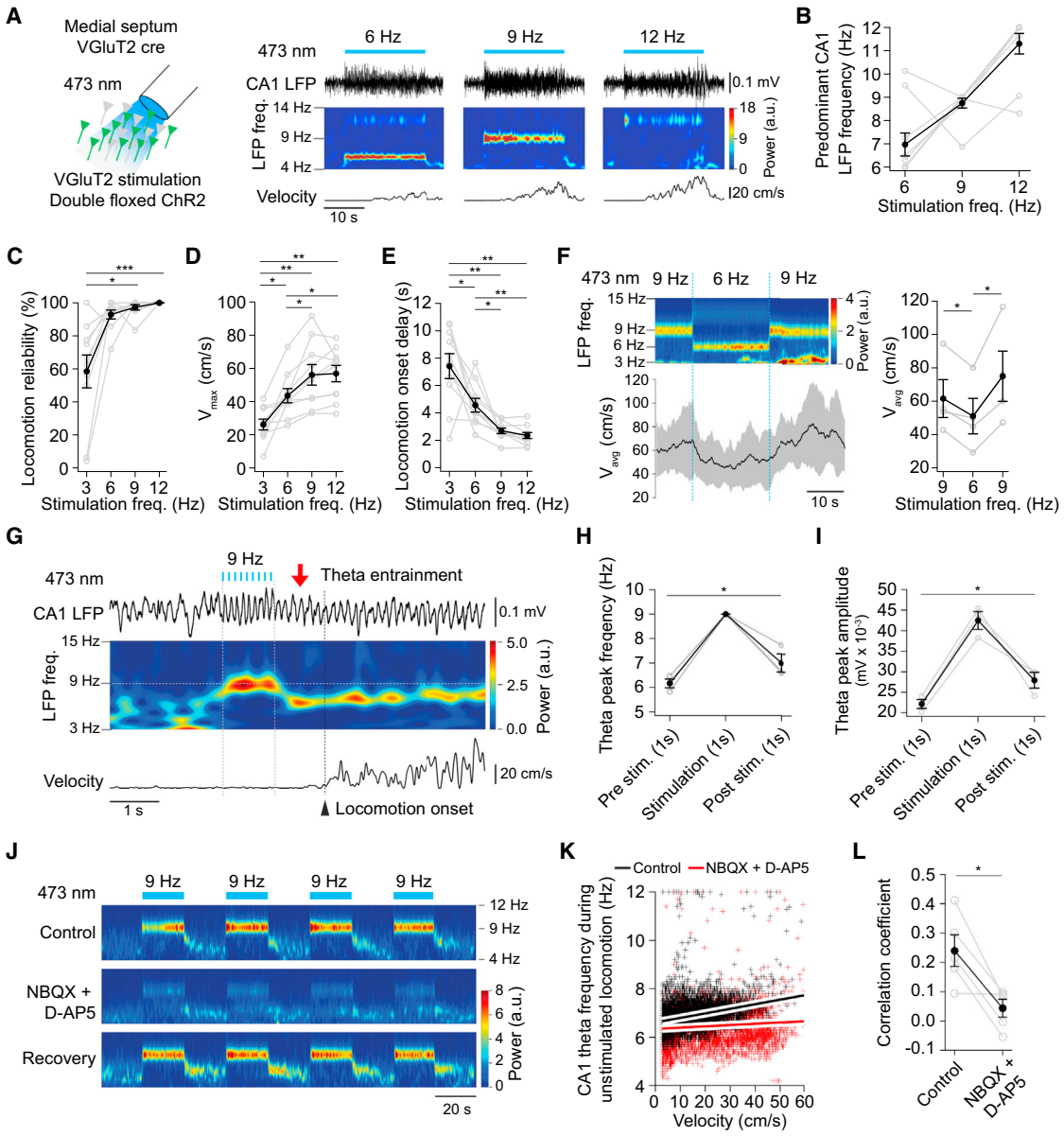

Figure 2. MSDB VGluT2 Neuronal Activity Initiates Locomotion, Controls Locomotion Velocity, and Entrains Hippocampal Oscillations

(A) Representative example of MSDB VGluT2-ChR2 stimulation-induced LFP oscillations in CA1 and locomotion at different frequencies.

(B) CA1 LFP oscillations match the stimulation frequencies (individual mouse data are presented in gray, n = 10 mice, mean values ± SEM).

(C–E) Reliability of locomotion initiation, locomotion velocity and the delay to locomotion onset depend on the stimulation frequency (n = 10 mice, mean values ± SEM).

(F) Transition of CA1 LFP oscillations and locomotion velocity in response to alternating stimulation frequencies (grand average of LFP spectrograms, gray area: SD of locomotion velocities, n = 4 mice, mean values ± SEM).

(G–I) Brief 1 s stimulation at 9 Hz effectively entrains endogenous (unstimulated) theta oscillations prior to the initiation of locomotion (n = 3 mice, mean ± SEM).

(J) Representative spectrograms (single mouse data) of CA1 LFP before, during, and 1 hr after local MSDB application of NBQX/D-AP5.

(K) Intraseptal glutamatergic blockade results in loss of the velocity-frequency correlation during unstimulated locomotion (single mouse data).

(L) NBQX/D-AP5 associated decrease in the correlation coefficient (n = 5 mice, mean ± SEM).

Also see Figure S2.

on the firing frequency of MSDB VGluT2 neurons (Figures 4A–4C). We observed an increase of CA1 population activity during voluntary locomotion in the absence of stimulation. However, the MSDB VGluT2 stimulation-dependent increase in Ca^{2+} transient frequency could be observed independently of locomotion, confirming that it directly depended on MSDB VGluT2 firing (Figure 4D). We then analyzed whether the observed VGluT2-frequency-dependent increase in population activity was consistent

Table 1. Mono-Transsynaptic Retrograde Tracing of MSDB VGluT2 Inputs

Brain Region	Number of Neurons per Brain Region, Mean ± SEM	Density, Mean ± SEM
Hypothalamus: Periventricular region/ zone		
Arcuate hypothalamic nucleus (ARH)	46 ± 34	97 ± 70 neurons/mm^2
Dorsomedial hypothalamic nucleus (DMH)	36 ± 19	31 ± 15 neurons/mm^2
Medial preoptic area (MPO)	539 ± 75	179 ± 25 neurons/mm^2
Median preoptic nucleus (MEPO)	101 ± 28	436 ± 121 neurons/mm^2
Paraventricular hypothalamic nucleus (PVH)	173 ± 128	320 ± 236 neurons/mm^2
Periventricular hypothalamic nucleus (PVpo, PVi)	85 ± 23	259 ± 64 neurons/mm^2
Hypothalamus: Hypothalamic medial zone		
Medial mammillary nucleus (MM)	18 ± 12	8 ± 5 neurons/mm^2
Posterior hypothalamic nucleus (PH)	38 ± 22	14 ± 8 neurons/mm^2
Premammillary nuclei (PM)	30 ± 12	50 ± 29 neurons/mm^2
Supramammillary nucleus lateral part (SUMl)	16 ± 10	23 ± 14 neurons/mm^2
Supramammillary nucleus medial part (SUMm)	23 ± 11	45 ± 21 neurons/mm^2
Ventromedial hypothalamic nucleus (VMH)	39 ± 23	30 ± 17 neurons/mm^2
Hypothalamus: Hypothalamic lateral zone		
Lateral hypothalamic area (LHA)	284 ± 165	21 ± 12 neurons/mm^2
Lateral preoptic area (LPO)	63 ± 19	21 ± 6 neurons/mm^2
Tubernal nucleus (TU)	68 ± 40	76 ± 43 neurons/mm^2
Pons		
Median raphe nucleus (MRN) (superior central nucleus raphe)	27 ± 1	31 ± 1 neurons/mm^2

Also see Figure S6.

with a more global mechanism acting on most neurons or a rather specific modulation of selected subpopulations of neurons. We plotted for all neurons the event frequency (9 Hz stimulation) against the unstimulated event frequency and observed that the increase in event frequencies was consistent with simulated data using a uniformly increased event rate (Figures 4E and 4F). This suggested a more global, unspecific increase of the activity of CA1 neurons.

Speed-Dependent Regulation of CA1 Input via Alveus/Oriens Interneuron Mediated Disinhibition

In several brain areas, disinhibitory interneuron-interneuron microcircuits control the activity of principal neurons during behavior (Fu et al., 2014). We found the strongest accumulation of VGluT2-EYFP-ChR2 axons in the alveus/oriens (A/O) region (Figure 5A) and hypothesized that local interneurons of the A/O subfield may represent a preferred synaptic target of septo-hippocampal VGluT2 axons (Klausberger and Somogyi, 2008). To test this directly, we stimulated the ChR2-expressing VGluT2 septo-hippocampal axons in acute hippocampal slices using field illumination with an optical fiber and performed whole-cell patch-clamp recordings of A/O interneurons. In the brain slice recordings monosynaptic input from VGluT2-ChR2 septo-hippocampal axons could be detected in 27.9% (64 of 229) A/O interneurons (Figures 5B and 5C, median delay 4.06 ms; Figure S4A). Excitatory postsynaptic potentials (EPSPs) were fully blocked by NBQX/D-AP5 (Figure 5C). We found that 2 out of 18 CA1 pyramidal neurons showed small stimulus-triggered EPSPs (delays: 22 and 5 ms, amplitudes: <0.5 mV), which raised the possibility that a small fraction of VGluT2-ChR2 septo-hippocampal axons may directly excite the dendritic compartment of pyramidal neurons. The post hoc recovered interneurons (8 out of 10 biocytin-filled A/O interneurons) were immuno-positive for somatostatin, identifying these neurons as putative oriens-lacunosum moleculare (O-LM) interneurons (Figure S4C; Klausberger and Somogyi, 2008). The MSDB VGluT2 axonal stimulation-evoked synaptic depolarization of A/O interneurons gradually increased with the stimulation frequency from 3 to 12 Hz (Figures 5D and 5E), suggesting that A/O interneurons increase their output firing with stronger VGluT2 input from the medial septum.

To test this in vivo in awake animals, we monitored the fluorescence of GCaMP6s-expressing A/O interneurons during VGluT-ChR2-stimulation induced locomotion on a linear treadmill using two-photon Ca^{2+} imaging. We found that A/O interneurons increased their fluorescence with higher stimulation frequencies, which is consistent with a discharge at higher rates (Figures 5F and 5G). We then monitored A/O interneuron activity during voluntary locomotion. We found that the GCaMP6s fluorescence of 132 out of 146 (90.4%) A/O interneurons strongly increased with locomotion (Figure S4D). Moreover, consistent with the activation patterns of MSDB VGluT2 neurons, the increase of fluorescence of locomotion-active A/O interneurons preceded the onset of movement, as was indicated by a significant increase in $\Delta F/F_0$ before locomotion onset (Figures 5H–5J).

We then asked how an increased activity of A/O interneurons could be translated into increased excitatory input to CA1 principal neurons during locomotion at higher velocities. Therefore, we selectively stimulated ChR2-eYFP expressing A/O interneurons using somatostatin (Sst)-cre mice. Action potential firing could be reliably evoked in A/O interneurons using light pulses of 3 ms duration (Figure S5). The electrophysiological profiles of the recorded neurons were consistent with O-LM interneurons (Gloveli et al., 2005; Table S1). O-LM interneurons have been recently shown to provide disinhibition by targeting local hippocampal feedforward interneurons (Leão et al., 2012). To find out whether a disinhibitory circuitry may be recruited in response to MSDB VGluT2 input, we stimulated ChR2-expressing A/O interneurons in brain slices of

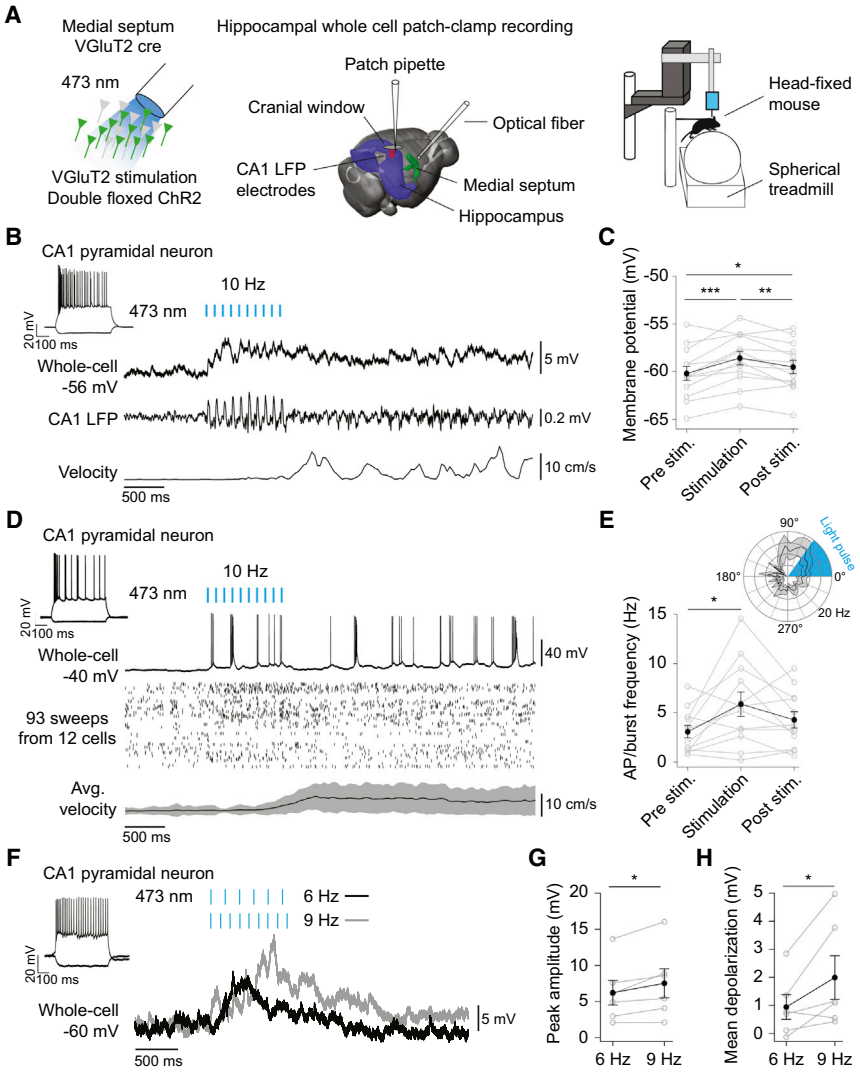

Figure 3. Stimulation-Locked Excitatory Input onto CA1 Pyramidal Neurons Increases with Higher MSDB VGluT2 Firing Frequencies

(A) Combined in vivo CA1 LFP and whole-cell patch-clamp recording configuration.

(B) Characteristic response pattern of a CA1 pyramidal cell to −200 pA and +500 pA current injections and response to 10 Hz MSDB VGluT2 stimulation.

(C) The membrane potential of a CA1 pyramidal neuron depolarizes in response to 10 Hz MSDB VGluT2-ChR2 stimulation (n = 13 neurons from 5 mice; mean ± SEM).

(D) Characteristic response pattern of a CA1 pyramidal cell to −200 pA and +500 pA current injections, response to 10 Hz MSDB VGluT2 stimulation, and the timing of APs/bursts recorded in 93 sweeps from 12 cells.

(E) Action potential firing rate of CA1 pyramidal neurons increases in response to 10 Hz MSDB VGluT2-ChR2 stimulation and is locked to the stimulation phase (n = 12 neurons from 5 mice; mean ± SEM).

(F) Characteristic response pattern of a CA1 pyramidal cell to −200 pA and +500 pA current injections and increasing subthreshold depolarization in response to increasing MSDB VGluT2 firing frequencies (from 6 Hz to 9 Hz)

(G and H) Peak and mean membrane potential depolarization increase with higher MSDB VGluT2 firing frequencies (n = 6 neurons in 3 mice; mean ± SEM).

Sst-cre mice while recording from feedforward interneurons in stratum radiatum (SR) and stratum lacunosum-moleculare (SLM). SR and SLM interneurons were classified as feedforward interneurons when they received monosynaptic EPSPs upon stimulation and showed electrophysiological profiles consistent with hippocampal feedforward interneurons (Elfant et al., 2008; Table S1: 66% of patched feedforward interneurons responded with monosynaptic inhibitory postsynaptic potentials [IPSPs] to A/O interneuron stimulation). When we paired electrical stimulation of either Schaffer collateral (CA3 input) or perforant path axons (MEC L3 input) with optogenetic activation of A/O interneurons in the hippocampal brain slice, the EPSPs evoked by both pathways were strongly curtailed (SR: by 59%, SLM: by 142%, Figures 6B–6D and 6H–6J). When stimulating A/O interneurons at theta frequencies, we observed a frequency-dependent inhibition of feedforward interneurons in SR and SLM (Figures 6E, 6F, 6K, and 6L), providing a global CA1 disinhibitory mechanism that links the integration of synaptic input of CA1 pyramidal neurons to the activity of MSDB-VGluT2 neurons.

DISCUSSION

Hippocampal oscillations and neuronal activity rates have long been known to depend on locomotion (McNaughton et al., 1983). However, the circuit mechanisms by which locomotion-related activity translates into speed-correlated neuronal activity have remained obscure along with the underlying circuitry. The present study reveals that the activity levels of hippocampal feedforward interneurons situated in both major CA1 input pathways (from entorhinal cortex and CA3) are controlled by locomotion-dependent inhibition. This disinhibitory mechanism is mediated via A/O interneurons, which integrate locomotion speed-dependent input from the MSDB via VGluT2 septo-hippocampal projections.

Entorhinal perforant path input from layer 3 to CA1 neuronal distal tuft dendrites is under strong feedforward and feedback inhibitory control (Ahmed and Mehta, 2009; Kitamura et al., 2014; Müller et al., 2012; Pouille and Scanziani, 2001; Royer et al., 2012). However, it has been demonstrated that perforant path input can evoke large EPSPs or nonlinear dendritic spikes/plateau potentials, which have been linked to the induction of synaptic plasticity and the transition of silent cells to place cells (Golding and Spruston, 1998; Golding et al., 2002; Lee et al., 2012; Takahashi and Magee, 2009). Under in vivo conditions of more predominant inhibition (Ahmed and Mehta,

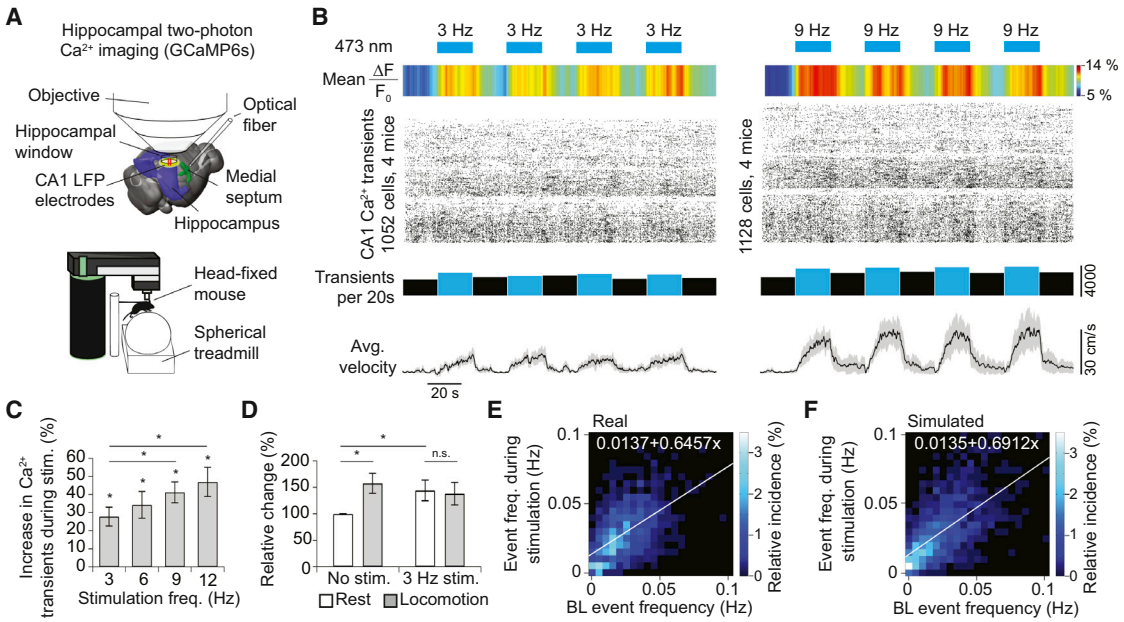

Figure 4. Hippocampal CA1 Population Activity Increases Uniformly with Higher MSDB VGluT2 Firing Frequencies

(A) In vivo two-photon imaging configuration.

(B) CA1 population mean fluorescence, GCaMP6s-Ca^{2+} event onsets and average locomotion velocities at 3 and 9 Hz MSDB VGluT2 stimulation (n = 4 mice, gray area represents SD).

(C) Frequency-dependent increase in the number of detected hippocampal GCaMP6s-Ca^{2+} transients (n = 4 mice, mean values ± SEM).

(D) CA1 population activity increases during voluntary locomotion, but the stimulation-dependent increase in hippocampal Ca^{2+} transient frequency can be evoked in the absence of locomotion (n = 4 mice, mean values ± SEM).

(E and F) The observed increase in event frequencies is consistent with simulated data assuming a uniform increase in event frequencies (Poisson processes with uniformly increased rates, bin size 0.005 × 0.005 Hz^2).

Also see Figure S3.

2009; English et al., 2014), e.g., during states associated with immobility, feedforward inhibition is expected to prevent the distal depolarization from propagating to the soma (Ang et al., 2005; Pouille and Scanziani, 2001). It has been demonstrated that synergistic, temporally overlapping inputs from CA3 onto proximal dendrites help to counteract dendritic inhibition, thus increasing axo-somatic depolarization and leading to the initiation of action potential firing (Jarsky et al., 2005).

We show that during a brain-state transition from immobility to locomotion an MSDB-VGluT2-mediated reduction of feedforward inhibition is acting on both Schaffer collateral and perforant path excitatory input streams. Thus, increased axo-somatic depolarization of CA1 pyramidal neurons would be expected to result from the reduced filtering of dendritic inputs. The locomotion speed-dependent reduction of input filtering via the MSDB-VGluT2-A/O interneuron circuit is consistent with the experimentally observed increase of the axo-somatic depolarization and neuronal activity with higher VGluT2 firing rates, which correlate to locomotion speed. This disinhibitory mechanism, which increases the sensitivity of CA1 pyramidal neurons to afferent input, could serve to compensate for the reduced sensory information per distance unit that can be integrated at higher speeds of locomotion.

All relevant elements of the intrahippocampal disinhibitory microcircuitry have been described in isolation. A/O interneurons (O-LM cells) have been shown to synapse onto local feedforward interneurons in SR (Leão et al., 2012). Likewise, experimental evidence suggests a disinhibitory synaptic connectivity with SLM-associated feedforward interneurons (Elfant et al., 2008). The VGluT2-mediated septo-hippocampal glutamatergic connectivity onto A/O interneurons has not been demonstrated yet, although the presence of this connection has been postulated (Huh et al., 2010).

It is possible that hippocampal pyramidal neurons in CA3 (Huh et al., 2010) and in CA1 (2/16 cells receive small-amplitude EPSPs in the present study) directly integrate some glutamatergic MSDB input, which could contribute to axo-somatic depolarization in a frequency-dependent manner. However, the glutamatergic EPSPs that were observed in acute preparations could be also explained by disinhibition of glutamatergic input deriving from spontaneous activity in CA3.

Further, there is evidence that A/O interneurons receive nicotinic input from the MSDB (Bell et al., 2011; Leão et al., 2012), which may be of particular importance during more immobility-associated sharp-wave states (Vandecasteele et al., 2014) and during contextual learning (Lovett-Barron et al., 2014). Given that intraseptal glutamatergic synapses onto cholinergic neurons have been reported (Leão et al., 2015; Manseau et al., 2005), it is possible that nicotinic synapses further contribute to excitation of A/O interneurons during locomotion.

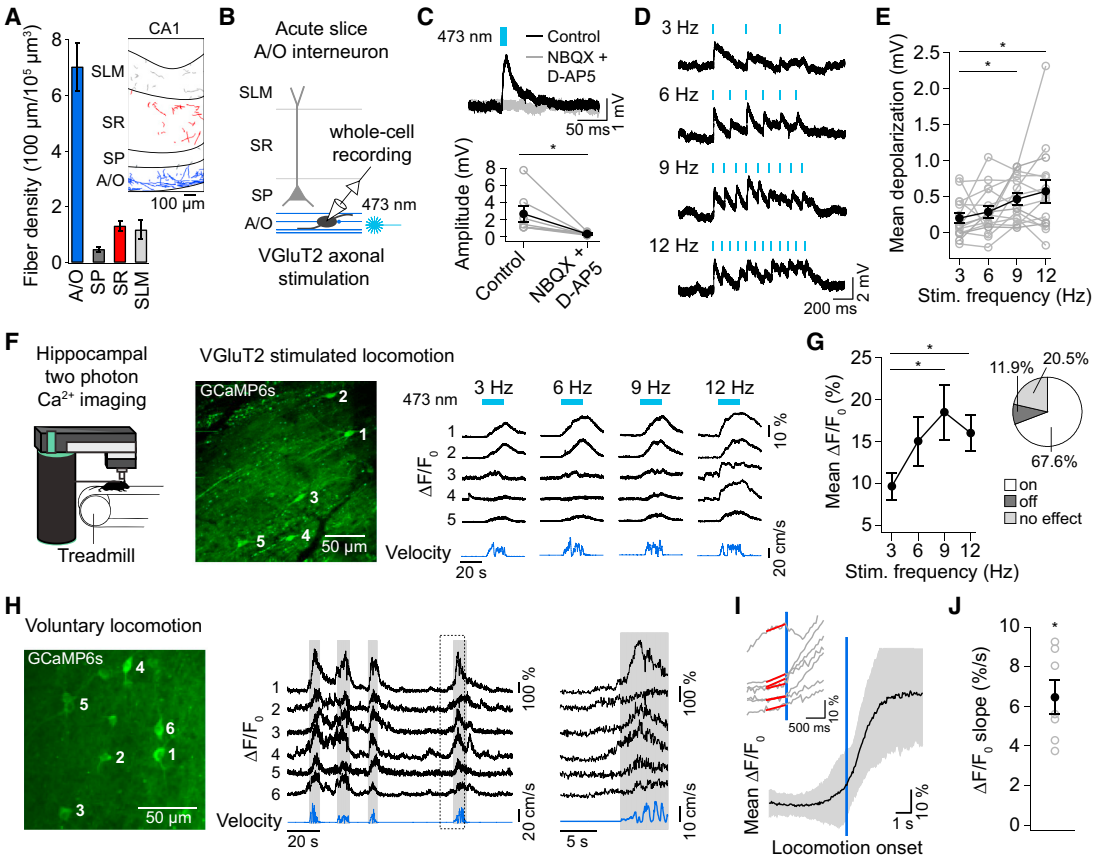

Figure 5. Hippocampal Alveus/Oriens Interneurons Integrate Locomotion-Dependent MSDB VGluT2 Input

(A) The density of septo-hippocampal glutamatergic fibers is highest in the alveus/oriens region. Inset: tracing of immunolabeled MSDB VGluT2-eYFP-ChR2 pos. axonal projections in subfield CA1.

(B) Brain slice whole-cell patch-clamp recordings from A/O interneurons with optical stimulation of VGluT2-ChR2 septo-hippocampal axons.

(C) Monosynaptic VGluT2-ChR2-evoked EPSPs are fully blocked by NBQX/D-AP5 (n = 7 cells individually displayed in gray, mean values ± SEM).

(D and E) Frequency-dependent summation of VGluT2-EPSPs and increase in mean depolarization of A/O interneurons in response to axonal stimulation at 3–12 Hz. (n = 15 cells, mean values ± SEM).

(F and G) In vivo two-photon imaging reveals frequency-dependent increases of somatic GCaMP6s fluorescence in response to MSDB VGluT2 stimulation from 3 to 12 Hz (frequency dependence was determined of 67.6% (125 of 185) A/O interneurons that were activated by MSDB VGluT2 stimulation).

(H) Somatic GCaMP6s fluorescence of A/O interneurons increases during voluntary locomotion (gray areas: locomotion intervals, dashed frame magnified in right panel).

(I) GCaMP6s fluorescence of A/O interneurons activated during locomotion increases prior to locomotion onset (n = 7 mice, gray area represents SD). Inset: average fluorescence obtained from the A/O interneuron population of 7 mice aligned to locomotion onset with a linear fit of the 500 ms interval preceding locomotion onset.

(J) Positive slope of the $\Delta F/F_0$ normalized fluorescence of A/O interneurons is detected during the 500 ms interval preceding the onset of locomotion (n = 7 mice, mean ± SEM).

Also see Figure S4.

Our mono-transsynaptic retrograde tracing identified several hypothalamic areas and the median raphe nucleus as main input regions to MSDB VGluT2 neurons (Bland and Oddie, 2001). These identified hypothalamic projection regions were distributed throughout the periventricular zone/region, the hypothalamic medial zone, and the lateral zone. Several of these hypothalamic nuclei, including the supramammillary nuclei, the periventricular nuclei, and the preoptic nuclei, have been identified as functional components of the diencephalic and mesencephalic locomotor zones (Sinnamon, 1993). Electrical and pharmacological stimulation (the latter avoiding stimulation of fibers of passage) of these regions initiated theta oscillations in the septohippocampal system and led to successful initiation of locomotion (Bland and Oddie, 2001; Oddie et al., 1996; Thinschmidt et al., 1995; Woodnorth and McNaughton, 2005). Notably, the initiation of locomotion and the evoked hippocampal theta oscillations were blocked when the medial septum was pharmacologically inactivated, suggesting a crucial role of the MSDB in both processes (Oddie et al., 1996).

Several lines of evidence support the notion that the execution of locomotion following VGluT2 stimulation is mediated via excitation of the ventral tegmental area (Oades and Halliday,

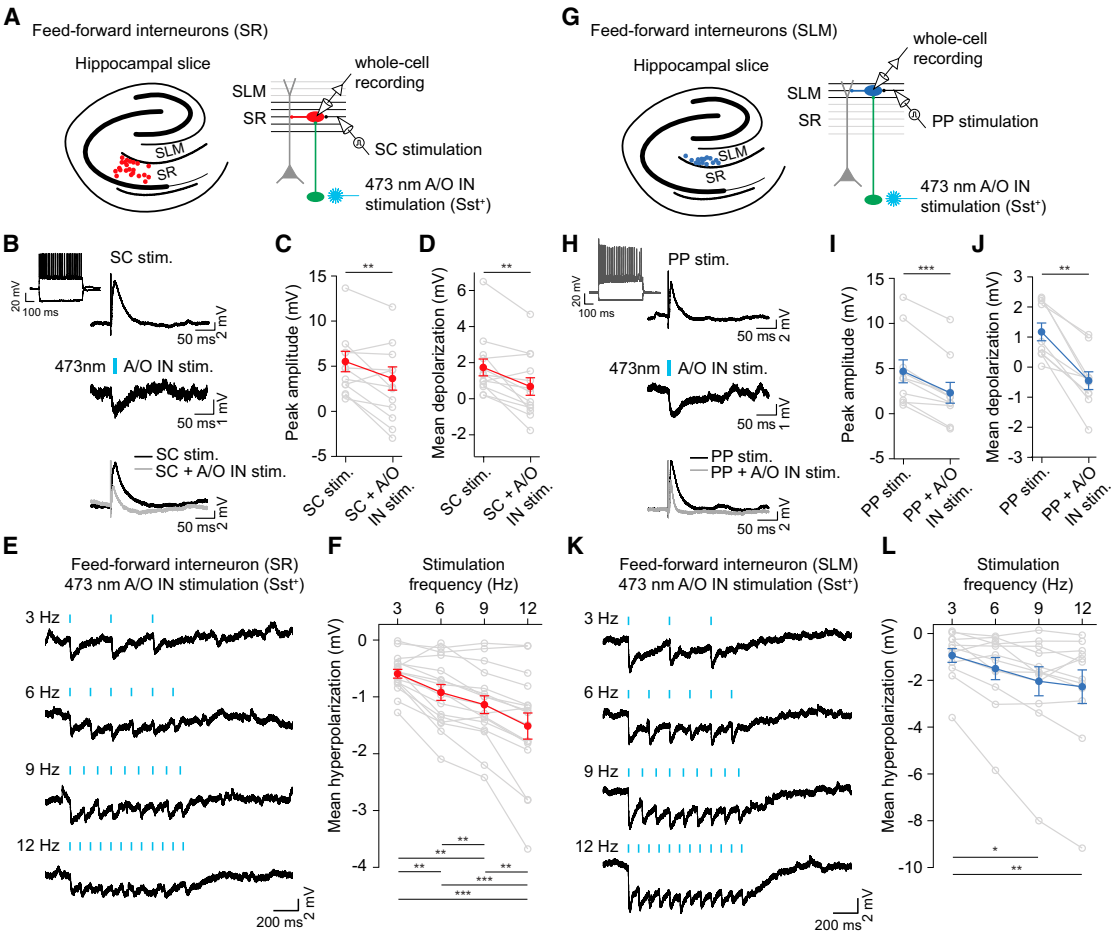

Figure 6. Firing of Hippocampal A/O Interneurons at Rhythmic VGluT2 Input Rates Suppresses Feedforward Inhibition in Both Main CA1 Input Pathways

(A) Locations of the recorded stratum radiatum (SR) feedforward interneurons (n = 22) within the hippocampal slices, responding with a monosynaptic EPSP to electrical Schaffer collateral (SC) stimulation and a monosynaptic IPSP to optical stimulation of ChR2 expressing Sst^+ A/O interneurons.

(B–D) SR feedforward interneurons identified by SC stimulation (EPSP) with characteristic response to −200 pA and +500 pA current injections, show reduced peak amplitude and mean depolarization when electrical stimulation is paired with optical A/O interneuron stimulation (n = 13 cells individually displayed in gray, mean values ± SEM).

(E and F) Mean hyperpolarization evoked by optical A/O interneuron stimulation increases with higher stimulation frequencies (n = 17 cells, mean values ± SEM).

(G) Locations of the recorded stratum lacunosum-moleculare (SLM) feedforward interneurons (n = 14) within the hippocampal slices, responding with a monosynaptic EPSP to electrical perforant path (PP) stimulation and a monosynaptic IPSP to optical stimulation of ChR2 expressing Sst^+ A/O interneurons.

(H–J) SLM feedforward interneurons identified by PP stimulation (EPSP) with characteristic response to −200 pA and +500 pA current injections, show reduced peak amplitude and mean depolarization when electrical stimulation is paired with optical A/O interneuron stimulation (n = 10 cells individually displayed in gray, mean values ± SEM).

(K and L) Mean hyperpolarization evoked by optical A/O interneuron stimulation increases with higher stimulation frequencies (n = 12 cells, mean values ± SEM). Also see Figure S5.

1987; Parker and Sinnamon, 1983; Sinnamon, 1993). (1) The firing rate of VTA non-dopaminergic and dopaminergic neurons strongly increases during the initiation of locomotion (Lee et al., 2001; Wang and Tsien, 2011) and the neuronal activity correlates with locomotion speed (Puryear et al., 2010; Wang and Tsien, 2011). (2) Electrical stimulation of VTA reliably initiates locomotion (Kalivas et al., 1981; Parker and Sinnamon, 1983). (3) The MSDB directly projects to VTA via VGluT2-positive axons (Geisler and Wise, 2008), a projection that was confirmed by axonal tracing in the present study. (4) VTA neurons modulate the excitability of nucleus accumbens (Mogenson et al., 1980) and motor cortex (Hosp et al., 2011; Kunori et al., 2014) and thus are probably involved in the generation of motor commands.

One important modulator of septo-hippocampal function is the median raphe nucleus (Varga et al., 2009), which has both afferent and efferent MSDB connections (see the present study and Vertes et al., 1999). It is associated with the inhibition of theta oscillations and motor activity. It has been shown that activation of median raphe neurons either blocked or desynchronized theta oscillations, while serotonergic blockade activated them (Maru

et al., 1979; Vertes et al., 1999). In addition, electrical and optogenetic stimulation of the raphe system led to behavioral inhibition and movement arrest (Fonseca et al., 2015; Steinfels et al., 1983).

Thus, efferent and afferent connectivity of the MSDB with hypothalamic locomotor regions, the median raphe nucleus—and the common projection to VTA (Geisler and Wise, 2008)—may promote the initiation and modulation of locomotion upon MSDB VGluT2 neuronal stimulation. Interestingly, these regions partially overlap with ascending brain stem pathways that have been associated with motivation and arousal (Mink et al., 1983; Moruzzi and Magoun, 1949).

Further supporting evidence for the speed-modulating action of the MSDB was provided by a recent study using muscimol for septal inactivation (Wang et al., 2015), which reduced the running speed during wheel running and during active navigation (but see Brandon et al., 2014). Likewise, upon medial septal heating, an increased oscillation frequency of MSDB neurons and increased running speed has been reported, while cooling had opposite effects (G. Buzsáki and E. Pastalkova, personal communication).

Together, our findings strongly suggest an important role of the MSDB-VGluT2 circuitry in the concerted initiation of locomotion and theta oscillations as well as in the active regulation of locomotion speed. Moreover, via activation of septo-hippocampal VGluT2 projections and the disinhibition of both major CA1 hippocampal input pathways, VGluT2 firing translates corollary information on the locomotor state into speed-correlated CA1 neuronal firing rates.

EXPERIMENTAL PROCEDURES

In Vivo Experimental Setup

For all in vivo experiments, habituated mice were placed on either a linear or spherical treadmill and were head fixed. Further connections for fluorometric monitoring or optical stimulation with simultaneous electrophysiological measurements or imaging were established. Locomotion of the mice was tracked by an optical computer mouse, which measured the rotation of the linear or spherical treadmill. Details of the experimental setups and transgenic mouse lines can be found in the Supplemental Experimental Procedures.

Fluorometric Monitoring

Stereotactic injection of AAV1.hSyn.Flex.GCaMP5G (GCaMP3-T302L.R303P.D380Y) WPRE.SV40, AV-1-PV2540 was used for local expression of GCaMP5 in MSDB VGluT2 neurons of VGluT2-cre mice. Ca^{2+} signals of MSDB VGluT2 neurons were monitored with a FiberOptoMeter coupled to an implanted fiber optic cannula delivering 470 nm excitation light into the MSDB and detecting the emitted activity-dependent fluorescence of MSDB VGluT2 neuronal population. Stereotactic coordinates, light fiber positioning, and surgery protocols can be found in the Supplemental Experimental Procedures.

In Vivo Optogenetic Stimulation

Stereotactic injections of pAAV2.1-EF1a-double floxed ChR2-EYFP-WPR (H134R) were used for local expression of ChR2 in MSDB VGluT2 neurons of VGluT2-cre mice. Light stimulation was performed with a 473 nm diode laser (Omicron-Laserage) coupled to an implanted fiber optic cannula. Detailed stimulation protocols can be found in the Supplemental Experimental Procedures. pcDNA3.1/hChR2(H134R)-EYFP was a gift from Karl Deisseroth (Addgene plasmid #20940).

In Vivo Electrophysiology

In all in vivo experiments hippocampal local field potentials were recorded using monopolar field potential electrodes positioned in hippocampal stratum radiatum. Whole-cell patch-clamp recordings were obtained from CA1 pyramidal cells in a depth of 1,000–1,400 μm from brain surface. Details of the in vivo recordings and the electrophysiological data acquisition and analysis can be found in the Supplemental Experimental Procedures.

In Vivo Two-Photon Hippocampal Imaging in Awake Mice

GCaMP6s was expressed in all hippocampal neurons by stereotatical injection of AAV1.Syn.GCaMP6s.WPRE into the right dorsal hippocampus. Two-photon imaging of hippocampal Ca^{2+} activity in awake mice on a treadmill was performed through an implanted hippocampal window using a resonant scanning microscope equipped with a Ti:sapphire laser. Image series of GCaMP fluorescence in either alveus/stratum oriens or stratum pyramidale were acquired at frame rates >15 Hz. Details of the surgery and the imaging acquisition/analysis can be found in the Supplemental Experimental Procedures.

Electrophysiological Recordings in Brain Slices

Whole-cell patch-clamp recordings were obtained from MSDB or hippocampal neurons in coronal and horizontal slices prepared from either VGluT2-cre mice expressing ChR2 in MSDB VGluT2 neurons or Sst-cre mice expressing ChR2 in hippocampal A/O interneurons. The ChR2 light stimulation of septo-hippocampal VGluT2 axons (VGluT2-cre) or A/O interneurons (Sst-cre) was performed using 473 nm illumination via an optical fiber. Hippocampal feedforward interneurons were identified by electrical stimulation of either Schaffer collateral or perforant path axons. Details of the slice preparation and the recording procedures can be found in the Supplemental Experimental Procedures.

Mono-Transsynaptic Retrograde Tracing

Injection of modified rAAVs and RABV into the MSDB of VGluT2-cre mice allowed for retrograde tracing of monosynaptic connection to MSDB VGluT2 neurons. Brain regions with retrogradely labeled neurons were identified using Allen Brain Atlas (Lein et al., 2007), available online from http://mouse.brain-map.org/. Details about the viral constructs, the injection and detailed images of labeled neurons throughout various brain regions can be found in the Supplemental Experimental Procedures.

Data Analysis and Statistics

All data were processed using custom written algorithms in MATLAB 2013 (The MathWorks) or Igor Pro 6.3 (WaveMetrics). All data were tested for normality using a Kolmogorov-Smirnov test and subsequently analyzed using an appropriate statistical test: paired t test or Wilcoxon rank test for two pairs of data and one-way ANOVA with post hoc Bonferroni test or Friedman with post hoc Dunn's test for multiple comparisons. Further details about the methods used for data processing and statistics can be found in the Supplemental Experimental Procedures.

SUPPLEMENTAL INFORMATION

Supplemental Information includes Supplemental Experimental Procedures, six figures, one table, and one movie and can be found with this article online at http://dx.doi.org/10.1016/j.neuron.2015.05.001.

AUTHOR CONTRIBUTIONS

F.F. performed the surgeries and in vivo imaging experiments, co-designed the hard- and software for all behavioral experiments, and wrote sections of the manuscript. D.J. performed the data analyses, statistical analyses, co-designed the hard- and software for all behavioral experiments, and wrote sections of the manuscript. L.S. and H.K. performed the in vivo and brain-slice patch-clamp experiments and analyzed brain-slice electrophysiology data. T.B. helped with imaging and electrophysiology data processing. D.F. performed immunohistochemistry and retrograde tracing analyses. S.S. produced and provided the viral vectors for optogenetic experiments. M.K.S. performed the monotranssynaptic retrograde tracing. M.F. provided technical support with the implementation of the chronic hippocampal window and

managed protocols for animal experiments. S.R. designed the experiments and wrote the manuscript.

ACKNOWLEDGMENTS

We thank György Buzsáki, Nelson Spruston, Viktor Varga, Marie Vandecasteele, and Mark Harnett for helpful comments on earlier versions of this manuscript. We thank Hongbo Jia for providing the FiberOptoMeter, Inna Schwarz for performing the RABV injections, Karl Klaus Conzelmann for the initial RABV inoculation, and the DZNE light microscopy facility for technical support. We thank the GENIE Project and the Janelia Farm Research Campus, specifically Vivek Jayaraman, Ph.D., Rex A. Kerr, Ph.D., Douglas S. Kim, Ph.D., Jasper Akerboom, Ph.D., Loren L. Looger, Ph.D., and Karel Svoboda, Ph.D. for providing GCaMP5 and GCaMP6. This work was supported by the Deutsche Forschungsgemeinschaft (SFB1089, S.R., M.F., M.K.S., S.S.).

Received: March 20, 2015
Revised: April 27, 2015
Accepted: April 29, 2015
Published: May 14, 2015

REFERENCES

Ahmed, O.J., and Mehta, M.R. (2009). The hippocampal rate code: anatomy, physiology and theory. Trends Neurosci. *32*, 329–338.

Andersen, P. (2007). The Hippocampus Book (Oxford: Oxford University Press).

Ang, C.W., Carlson, G.C., and Coulter, D.A. (2005). Hippocampal CA1 circuitry dynamically gates direct cortical inputs preferentially at theta frequencies. J. Neurosci. *25*, 9567–9580.

Bell, K.A., Shim, H., Chen, C.K., and McQuiston, A.R. (2011). Nicotinic excitatory postsynaptic potentials in hippocampal CA1 interneurons are predominantly mediated by nicotinic receptors that contain α4 and β2 subunits. Neuropharmacology *61*, 1379–1388.

Bland, B.H., and Oddie, S.D. (2001). Theta band oscillation and synchrony in the hippocampal formation and associated structures: the case for its role in sensorimotor integration. Behav. Brain Res. *127*, 119–136.

Brandon, M.P., Koenig, J., Leutgeb, J.K., and Leutgeb, S. (2014). New and distinct hippocampal place codes are generated in a new environment during septal inactivation. Neuron *82*, 789–796.

Buzsáki, G. (2002). Theta oscillations in the hippocampus. Neuron *33*, 325–340.

Buzsáki, G., Leung, L.W., and Vanderwolf, C.H. (1983). Cellular bases of hippocampal EEG in the behaving rat. Brain Res. *287*, 139–171.

Colom, L.V., Castaneda, M.T., Reyna, T., Hernandez, S., and Garrido-Sanabria, E. (2005). Characterization of medial septal glutamatergic neurons and their projection to the hippocampus. Synapse *58*, 151–164.

Czurkó, A., Hirase, H., Csicsvari, J., and Buzsáki, G. (1999). Sustained activation of hippocampal pyramidal cells by 'space clamping' in a running wheel. Eur. J. Neurosci. *11*, 344–352.

Ekstrom, A.D., Meltzer, J., McNaughton, B.L., and Barnes, C.A. (2001). NMDA receptor antagonism blocks experience-dependent expansion of hippocampal "place fields". Neuron *31*, 631–638.

Elfant, D., Pál, B.Z., Emptage, N., and Capogna, M. (2008). Specific inhibitory synapses shift the balance from feedforward to feedback inhibition of hippocampal CA1 pyramidal cells. Eur. J. Neurosci. *27*, 104–113.

English, D.F., Peyrache, A., Stark, E., Roux, L., Vallentin, D., Long, M.A., and Buzsáki, G. (2014). Excitation and inhibition compete to control spiking during hippocampal ripples: intracellular study in behaving mice. J. Neurosci. *34*, 16509–16517.

Fonseca, M.S., Murakami, M., and Mainen, Z.F. (2015). Activation of dorsal raphe serotonergic neurons promotes waiting but is not reinforcing. Curr. Biol. *25*, 306–315.

Freund, T.F., and Antal, M. (1988). GABA-containing neurons in the septum control inhibitory interneurons in the hippocampus. Nature *336*, 170–173.

Frotscher, M., and Léránth, C. (1985). Cholinergic innervation of the rat hippocampus as revealed by choline acetyltransferase immunocytochemistry: a combined light and electron microscopic study. J. Comp. Neurol. *239*, 237–246.

Fu, Y., Tucciarone, J.M., Espinosa, J.S., Sheng, N., Darcy, D.P., Nicoll, R.A., Huang, Z.J., and Stryker, M.P. (2014). A cortical circuit for gain control by behavioral state. Cell *156*, 1139–1152.

Geisler, S., and Wise, R.A. (2008). Functional implications of glutamatergic projections to the ventral tegmental area. Rev. Neurosci. *19*, 227–244.

Gloveli, T., Dugladze, T., Saha, S., Monyer, H., Heinemann, U., Traub, R.D., Whittington, M.A., and Buhl, E.H. (2005). Differential involvement of oriens/pyramidale interneurones in hippocampal network oscillations in vitro. J. Physiol. *562*, 131–147.

Golding, N.L., and Spruston, N. (1998). Dendritic sodium spikes are variable triggers of axonal action potentials in hippocampal CA1 pyramidal neurons. Neuron *21*, 1189–1200.

Golding, N.L., Staff, N.P., and Spruston, N. (2002). Dendritic spikes as a mechanism for cooperative long-term potentiation. Nature *418*, 326–331.

Green, J.D., and Arduini, A.A. (1954). Hippocampal electrical activity in arousal. J. Neurophysiol. *17*, 533–557.

Hangya, B., Borhegyi, Z., Szilágyi, N., Freund, T.F., and Varga, V. (2009). GABAergic neurons of the medial septum lead the hippocampal network during theta activity. J. Neurosci. *29*, 8094–8102.

Hosp, J.A., Pekanovic, A., Rioult-Pedotti, M.S., and Luft, A.R. (2011). Dopaminergic projections from midbrain to primary motor cortex mediate motor skill learning. J. Neurosci. *31*, 2481–2487.

Huh, C.Y., Goutagny, R., and Williams, S. (2010). Glutamatergic neurons of the mouse medial septum and diagonal band of Broca synaptically drive hippocampal pyramidal cells: relevance for hippocampal theta rhythm. J. Neurosci. *30*, 15951–15961.

Jarsky, T., Roxin, A., Kath, W.L., and Spruston, N. (2005). Conditional dendritic spike propagation following distal synaptic activation of hippocampal CA1 pyramidal neurons. Nat. Neurosci. *8*, 1667–1676.

Kalivas, P.W., Nemeroff, C.B., and Prange, A.J., Jr. (1981). Increase in spontaneous motor activity following infusion of neurotensin into the ventral tegmental area. Brain Res. *229*, 525–529.

King, C., Recce, M., and O'Keefe, J. (1998). The rhythmicity of cells of the medial septum/diagonal band of Broca in the awake freely moving rat: relationships with behaviour and hippocampal theta. Eur. J. Neurosci. *10*, 464–477.

Kitamura, T., Pignatelli, M., Suh, J., Kohara, K., Yoshiki, A., Abe, K., and Tonegawa, S. (2014). Island cells control temporal association memory. Science *343*, 896–901.

Klausberger, T., and Somogyi, P. (2008). Neuronal diversity and temporal dynamics: the unity of hippocampal circuit operations. Science *321*, 53–57.

Köhler, C., Chan-Palay, V., and Wu, J.Y. (1984). Septal neurons containing glutamic acid decarboxylase immunoreactivity project to the hippocampal region in the rat brain. Anat. Embryol. (Berl.) *169*, 41–44.

Kunori, N., Kajiwara, R., and Takashima, I. (2014). Voltage-sensitive dye imaging of primary motor cortex activity produced by ventral tegmental area stimulation. J. Neurosci. *34*, 8894–8903.

Leão, R.N., Mikulovic, S., Leão, K.E., Munguba, H., Gezelius, H., Enjin, A., Patra, K., Eriksson, A., Loew, L.M., Tort, A.B., and Kullander, K. (2012). OLM interneurons differentially modulate CA3 and entorhinal inputs to hippocampal CA1 neurons. Nat. Neurosci. *15*, 1524–1530.

Leão, R.N., Targino, Z.H., Colom, L.V., and Fisahn, A. (2015). Interconnection and synchronization of neuronal populations in the mouse medial septum/diagonal band of Broca. J. Neurophysiol. *113*, 971–980.

Lee, R.S., Steffensen, S.C., and Henriksen, S.J. (2001). Discharge profiles of ventral tegmental area GABA neurons during movement, anesthesia, and the sleep-wake cycle. J. Neurosci. *21*, 1757–1766.

Lee, D., Lin, B.J., and Lee, A.K. (2012). Hippocampal place fields emerge upon single-cell manipulation of excitability during behavior. Science *337*, 849–853.

Lein, E.S., Hawrylycz, M.J., Ao, N., Ayres, M., Bensinger, A., Bernard, A., Boe, A.F., Boguski, M.S., Brockway, K.S., Byrnes, E.J., et al. (2007). Genome-wide atlas of gene expression in the adult mouse brain. Nature *445*, 168–176.

Léránth, C., and Frotscher, M. (1987). Cholinergic innervation of hippocampal GAD- and somatostatin-immunoreactive commissural neurons. J. Comp. Neurol. *261*, 33–47.

Lovett-Barron, M., Kaifosh, P., Kheirbek, M.A., Danielson, N., Zaremba, J.D., Reardon, T.R., Turi, G.F., Hen, R., Zemelman, B.V., and Losonczy, A. (2014). Dendritic inhibition in the hippocampus supports fear learning. Science *343*, 857–863.

Manseau, F., Danik, M., and Williams, S. (2005). A functional glutamatergic neurone network in the medial septum and diagonal band area. J. Physiol. *566*, 865–884.

Maru, E., Takahashi, L.K., and Iwahara, S. (1979). Effects of median raphe nucleus lesions on hippocampal EEG in the freely moving rat. Brain Res. *163*, 223–234.

McFarland, W.L., Teitelbaum, H., and Hedges, E.K. (1975). Relationship between hippocampal theta activity and running speed in the rat. J. Comp. Physiol. Psychol. *88*, 324–328.

McNaughton, B.L., Barnes, C.A., and O'Keefe, J. (1983). The contributions of position, direction, and velocity to single unit activity in the hippocampus of freely-moving rats. Exp. Brain Res. *52*, 41–49.

Mink, J.W., Sinnamon, H.M., and Adams, D.B. (1983). Activity of basal forebrain neurons in the rat during motivated behaviors. Behav. Brain Res. *8*, 85–108.

Mogenson, G.J., Jones, D.L., and Yim, C.Y. (1980). From motivation to action: functional interface between the limbic system and the motor system. Prog. Neurobiol. *14*, 69–97.

Moruzzi, G., and Magoun, H.W. (1949). Brain stem reticular formation and activation of the EEG. Electroencephalogr. Clin. Neurophysiol. *1*, 455–473.

Müller, C., Beck, H., Coulter, D., and Remy, S. (2012). Inhibitory control of linear and supralinear dendritic excitation in CA1 pyramidal neurons. Neuron *75*, 851–864.

Oades, R.D., and Halliday, G.M. (1987). Ventral tegmental (A10) system: neurobiology. 1. Anatomy and connectivity. Brain Res. *434*, 117–165.

Oddie, S.D., Stefanek, W., Kirk, I.J., and Bland, B.H. (1996). Intraseptal procaine abolishes hypothalamic stimulation-induced wheel-running and hippocampal theta field activity in rats. J. Neurosci. *16*, 1948–1956.

Parker, S.M., and Sinnamon, H.M. (1983). Forward locomotion elicited by electrical stimulation in the diencephalon and mesencephalon of the awake rat. Physiol. Behav. *31*, 581–587.

Pouille, F., and Scanziani, M. (2001). Enforcement of temporal fidelity in pyramidal cells by somatic feed-forward inhibition. Science *293*, 1159–1163.

Puryear, C.B., Kim, M.J., and Mizumori, S.J. (2010). Conjunctive encoding of movement and reward by ventral tegmental area neurons in the freely navigating rodent. Behav. Neurosci. *124*, 234–247.

Royer, S., Zemelman, B.V., Losonczy, A., Kim, J., Chance, F., Magee, J.C., and Buzsáki, G. (2012). Control of timing, rate and bursts of hippocampal place cells by dendritic and somatic inhibition. Nat. Neurosci. *15*, 769–775.

Sinnamon, H.M. (1993). Preoptic and hypothalamic neurons and the initiation of locomotion in the anesthetized rat. Prog. Neurobiol. *41*, 323–344.

Steinfels, G.F., Heym, J., Strecker, R.E., and Jacobs, B.L. (1983). Raphe unit activity in freely moving cats is altered by manipulations of central but not peripheral motor systems. Brain Res. *279*, 77–84.

Stumpf, C., Petsche, H., and Gogolak, G. (1962). The significance of the rabbit's septum as a relay station between the midbrain and the hippocampus. II. The differential influence of drugs upon both the septal cell firing pattern and the hippocampus theta activity. Electroencephalogr. Clin. Neurophysiol. *14*, 212–219.

Takahashi, H., and Magee, J.C. (2009). Pathway interactions and synaptic plasticity in the dendritic tuft regions of CA1 pyramidal neurons. Neuron *62*, 102–111.

Thinschmidt, J.S., Kinney, G.G., and Kocsis, B. (1995). The supramammillary nucleus: is it necessary for the mediation of hippocampal theta rhythm? Neuroscience *67*, 301–312.

Tóth, K., Freund, T.F., and Miles, R. (1997). Disinhibition of rat hippocampal pyramidal cells by GABAergic afferents from the septum. J. Physiol. *500*, 463–474.

Vandecasteele, M., Varga, V., Berényi, A., Papp, E., Barthó, P., Venance, L., Freund, T.F., and Buzsáki, G. (2014). Optogenetic activation of septal cholinergic neurons suppresses sharp wave ripples and enhances theta oscillations in the hippocampus. Proc. Natl. Acad. Sci. USA *111*, 13535–13540.

Vanderwolf, C.H. (1969). Hippocampal electrical activity and voluntary movement in the rat. Electroencephalogr. Clin. Neurophysiol. *26*, 407–418.

Varga, V., Losonczy, A., Zemelman, B.V., Borhegyi, Z., Nyiri, G., Domonkos, A., Hangya, B., Holderith, N., Magee, J.C., and Freund, T.F. (2009). Fast synaptic subcortical control of hippocampal circuits. Science *326*, 449–453.

Vertes, R.P., Fortin, W.J., and Crane, A.M. (1999). Projections of the median raphe nucleus in the rat. J. Comp. Neurol. *407*, 555–582.

Wang, D.V., and Tsien, J.Z. (2011). Conjunctive processing of locomotor signals by the ventral tegmental area neuronal population. PLoS ONE *6*, e16528.

Wang, Y., Romani, S., Lustig, B., Leonardo, A., and Pastalkova, E. (2015). Theta sequences are essential for internally generated hippocampal firing fields. Nat. Neurosci. *18*, 282–288.

Whishaw, I.Q., and Vanderwolf, C.H. (1973). Hippocampal EEG and behavior: changes in amplitude and frequency of RSA (theta rhythm) associated with spontaneous and learned movement patterns in rats and cats. Behav. Biol. *8*, 461–484.

Woodnorth, M.A., and McNaughton, N. (2005). Different systems in the posterior hypothalamic nucleus of rats control theta frequency and trigger movement. Behav. Brain Res. *163*, 107–114.

Wyble, B.P., Hyman, J.M., Rossi, C.A., and Hasselmo, M.E. (2004). Analysis of theta power in hippocampal EEG during bar pressing and running behavior in rats during distinct behavioral contexts. Hippocampus *14*, 662–674.